

# Face Swapping as A Simple Arithmetic Operation

Truong Vu<sup>1</sup>

truong.vt183649@sis.hust.edu.vn

Kien Do<sup>2</sup>

k.do@deakin.edu.au

Khang Nguyen<sup>1</sup>

khang.nt183559@sis.hust.edu.vn

Khoat Than<sup>1</sup>

khoattq@soict.hust.edu.vn

<sup>1</sup> Hanoi University of Science and Technology, Vietnam

<sup>2</sup> Applied Artificial Intelligence Institute (A2I2), Deakin University, Australia

## Abstract

*We propose a novel high-fidelity face swapping method called “Arithmetic Face Swapping” (AFS) that explicitly disentangles the intermediate latent space  $\mathcal{W}^+$  of a pre-trained StyleGAN into the “identity” and “style” subspaces so that a latent code in  $\mathcal{W}^+$  is the sum of an “identity” code and a “style” code in the corresponding subspaces. Via our disentanglement, face swapping (FS) can be regarded as a simple arithmetic operation in  $\mathcal{W}^+$ , i.e., the summation of a source “identity” code and a target “style” code. This makes AFS more intuitive and elegant than other FS methods. In addition, our method can generalize over the standard face swapping to support other interesting operations, e.g., combining the identity of one source with styles of multiple targets and vice versa. We implement our identity-style disentanglement by learning a neural network that maps a latent code to a “style” code. We provide a condition for this network which theoretically guarantees identity preservation of the source face even after a sequence of face swapping operations. Extensive experiments demonstrate the advantage of our method over state-of-the-art FS methods in producing high-quality swapped faces. Our source code was made public at <https://github.com/truongvu2000nd/AFS>*

## 1. Introduction

Face swapping is the task of transferring the identity from a source face image to a target face image while preserving the attributes (styles) of the target face image such as pose, facial expression, lighting, and background. It has attracted a lot of attentions from community recently thanks to its practical applications in entertainment [9, 23] and privacy protection [36].

A large number of face swapping methods have been proposed. Early methods can only handle source and target

faces with similar poses, or source faces with known identities [6, 25]. Later methods are able to deal with source and target faces having very different styles, and can even work in unconstrained settings [4, 9, 27, 30, 31]. Among them, GAN-based methods [9, 27] often achieve better visual results than those using conventional image blending models [30, 31].

Recent years have also witnessed the development of several powerful GANs for image generation [8, 20–22]. StyleGAN [21, 22] is probably the current state-of-the-art, which been shown to be capable of generating diverse high-fidelity images at megapixel resolution. Its superiority mainly comes from the original architectural design of its generator. In conventional GANs [16], an input noise vector  $z \in \mathcal{Z}$  directly passes through the generator  $G$  in a feed-forward manner. Meanwhile, in StyleGAN,  $z$  is mapped to an intermediate latent code  $w \in \mathcal{W}$  which is then used to modulate the intermediate feature maps of  $G$  at different spatial resolutions. Many works have shown that the latent space  $\mathcal{W}^+$  of StyleGAN - an extension of  $\mathcal{W}$  - is more expressive and disentangled than  $\mathcal{W}$  and  $\mathcal{Z}$ , motivating the use of  $\mathcal{W}^+$  for latent space manipulation [1, 2].

Inspired by the great capability of StyleGAN, several works have made use of a pretrained StyleGAN to perform high-resolution face swapping. Zhu et al. [56] proposed to learn a Face Transfer Module (FTM) that combines the inverted latent codes of the source and target faces to obtain a swapped latent code which will then be sent to the StyleGAN generator to produce a swapped face. However, since the two latent codes contain entangled information of identity and attributes, directly fusing them together may cause the swapped result to retain some information of the source attributes and the target identity. Xu et al. [50], on the other hand, proposed to concatenate the “structure” part of the source latent code with the disjoint “appearance” part of the target latent code to get an input latent code for the StyleGAN generator. Unfortunately, this input latent code still

contains entangled information in its parts. Thus, the generated face derived from it has mixed styles, and is considered as a side output not the final result.

To address the above limitation, we propose a novel face swapping method based on a pretrained StyleGAN that explicitly disentangles the intermediate latent space  $\mathcal{W}^+$  of a pretrained StyleGAN into two *subspaces*  $\mathcal{W}_{id}^+$  and  $\mathcal{W}_{sty}^+$  characterizing identity and style respectively. Motivated by the expressiveness and linear editability of  $\mathcal{W}^+$  [1, 44], we hypothesize that we can represent the inverted latent code  $w \in \mathcal{W}^+$  of a face image as the sum of an “identity” code  $w_{id} \in \mathcal{W}_{id}^+$  and a “style” code  $w_{sty} \in \mathcal{W}_{sty}^+$ , i.e.,  $w = w_{id} + w_{sty}$ . This enables us to regard face swapping as a simple *arithmetic operation* in  $\mathcal{W}^+$ , that is the summation of a *source* “identity” code and a *target* “style” code. Therefore, we name our method “Arithmetic Face Swapping” (AFS). Compared to existing formulations of face swapping, ours is more intuitive and elegant. In fact, the standard face swapping is just a *special case* of numerous operations that our identity-style disentanglement could support. For example, we can take the (weighted) average of multiple target style codes in  $\mathcal{W}_{sty}^+$  and combine the result with a source identity code in  $\mathcal{W}_{id}^+$  via summation, which is equivalent to face swapping with one identity and multiple styles. Similarly, we can easily combine multiple identities together to create a new identity that has not existed before without changing styles. These kinds of face swapping, to the best of our knowledge, have never been considered in previous works. We implement our identity-style disentanglement by learning a style extractor network  $h$  that maps  $w$  to  $w_{sty}$  and compute  $w_{id}$  as  $w - h(w)$ . We also provide a condition for  $h$  which theoretically guarantees that our method can preserve the identity of the source image even when this image goes through a sequence of face swapping operations with different styles. This condition is then turned into an objective for training  $h$ , along with other well-designed objectives to ensure that  $w_{id}$  and  $w_{sty}$  derived from  $h$  capture the true identity and style information in  $w$  respectively. Extensive experiments demonstrate that AFS outperforms existing state-of-the-art face swapping methods in generating high-quality results, and preserving the source identity and the target attributes.

## 2. Related Work

**Face Swapping** Face swapping has long been an interesting and difficult problem in computer vision [7]. Early approaches are mainly based on conventional image processing techniques, thus, require the source and target faces to have similar poses and appearances [6, 47]. With the development deep neural networks, especially deep generative models such as VAEs [24] and GANs [16], more advanced face swapping methods have been proposed. Korshunova et al. [25] regard face swapping as a style transfer problem

in which content is the target face, and style is the source identity. They leverage a Texture Network [45] to model the identity of each subject in the training data. However, their method cannot generalize to unseen subjects. Nirkin et al. [31] learn an occlusion-aware face segmentation model and combine it with off-the-shelf 3D morphable face models (3DMM) [32, 55] and image blending model [34] to form a complete pipeline for face swapping that can handle unconstrained face images. Their subsequent work [30] further enhances this pipeline by proposing a novel reenactment generator to better preserve the target pose and expression, and a novel blending loss to better preserve the target skin color. However, due to the limitation of the Possion blender in simulating complex textures and lighting effects, methods based on this technique [30, 31, 36] tend to create unnatural swapped faces. Therefore, there has been another line of works that make use of GANs to generate real looking swapped faces. FSNet [29] extracts the representation of the source face region and the representation of the target face landmarks, and sends them along with the target face-masked image to an UNet-like generator to generate a swapped face. Since only the target landmark information is given as input to the generator, this model may not be able to preserve the expression and skin color of the target face. IP-GAN [4] generates a swapped face from the concatenation of the source identity and the target attribute vectors. This method can generalize to unseen identities quite well but often fails to preserve details in the target face such as wrinkles or beards. FaceShifter [27] proposes a well-designed generator that combines the source identity vector with the target attribute feature maps at various spatial resolutions. This generator can generate good-looking a swapped face that faithfully respects the style and resolution of the target face. The swapped face then goes through a refinement network for facial occlusion correction. SimSwap [9] uses an ID Injection Module (IIM) to integrate the source identity into the target features before sending to the generator. This IIM contains multiple AdaIN layers [19] whose parameters depend on the source identity. HiFiFace [48] extends the source identity vector with the target 3D pose and expression representation vectors extracted by a 3DMM model [12], and uses this extended source identity vector to modulate the generation of a swapped face from the target face in nearly the same way as FaceShifter. FaceInpainter [26] is a two-stage face swapping framework inspired by FaceShifter that also uses 3D pose and expression as prior knowledge for face swapping. InfoSwap [14] leverages the Information Bottleneck principle [3] to achieve a good separation between identity and style information.

Besides the aforementioned methods, some methods make use of a pretrained StyleGAN2 and are more related to ours. These methods usually map the source and the target faces to the StyleGAN2 intermediate latent codes, and use

these latent codes to perform face swapping. MegaFS [56] uses a Face Transfer Module (FTM) to fuse 14 high-level components of the source and the target latent codes together. The fused high-level components are then concatenated with the remaining 4 low-level components of the target latent codes to obtain a complete swapped latent code which serves as the input to the StyleGAN2 generator to generate a swapped face. HiRes [50] uses both the source and the target facial landmarks to modify the “structure” part of the source latent codes (consisting of the first 7 components), and combines the modified one with the “appearance” part of the target latent codes (consisting of the last 11 components) to obtain a swapped latent code. This swapped latent code is then fed to the StyleGAN2 generator not to generate a swapped face but to get the intermediate feature maps. These intermediate feature maps will be used to modulate another auto-encoder network that maps the target face to the actual swapped face.

### GAN Inversion and GAN Latent Space Manipulation

Due to large scopes of GAN Inversion and GAN Latent Space Manipulation, in this paper, we only discuss works in these topics that are the most related to ours. Given a well-trained GAN, we often want to find the latent code that faithfully represents an input image. There are three main approaches to the problem namely i) latent optimization [1, 2, 10, 28], ii) learning an encoder [33, 35, 44], and iii) the hybrid of learning an encoder and latent optimization [5, 54]. The first approach directly optimizes a random latent code by minimizing the reconstruction error between the generated image w.r.t. the latent code and the input image. This approach often yields accurate inversion but does not scale well since we have to run multiple optimization steps for each input image. By contrast, the second approach computes the latent code via a single forward pass through the encoder, thus, is significantly faster at inference time. The third approach learns an encoder to find good initializations of latent codes, then optimizes these latent initializations. This approach often enjoys the benefits of fast inference and good accuracy from the first two approaches.

Many recent works have shown that semantically meaningful image editions can be done via simple affine transformations in the latent space of a pretrained GAN. Some works try to discover interpretable directions in the GAN latent space in an unsupervised manner [17, 39, 46]. However, they have to manually assign semantics to the discovered directions. Supervised methods [38, 42, 43, 51], by contrast, make use of pretrained attribute classifiers/regressors to guide the search for semantic directions.

## 3. Method

Since our method makes use of a pretrained StyleGAN2 [22] for face swapping, below we give a brief description

of StyleGAN [21] and StyleGAN2 [22] before going into details of our method.

### 3.1. StyleGAN and StyleGAN2

StyleGAN [21] is a recent state-of-the-art variant of GANs [16] that is able to generate high-fidelity images at high resolution. Its generator  $G$  inherits many advantageous designs from the style transfer literature [19]. Different from conventional GANs, in StyleGAN, the noise vector  $z \in \mathcal{Z}$  is not fed directly to  $G$  but is mapped to an *intermediate* latent code  $w \in \mathcal{W} \subset \mathbb{R}^{512}$  via an 8-layer MLP  $f : \mathcal{Z} \rightarrow \mathcal{W}$ . This latent code  $w$  controls the style and other details of a generated image from coarse to fine levels by serving as input to 18 different AdaIN layers [13, 15, 19] of the generator at various spatial resolutions from  $4 \times 4$  to  $1024 \times 1024$  (2 AdaIN layers for each spatial resolution). Several works [17, 38] empirically showed that  $\mathcal{W}$  supports linear latent code manipulation as they were able to find semantic directions in  $\mathcal{W}$  corresponding to meaningful disentangled attributes such as color change, zoom, pose, gender, etc. However,  $\mathcal{W}$  is still not expressive enough to support faithful reconstruction of existing images [1, 2, 35]. Therefore, later works mostly consider the *extended* latent space  $\mathcal{W}^+$  rather than  $\mathcal{W}$  for image editing and face swapping tasks [42, 44, 50, 56]. An *extended* latent code  $w \in \mathcal{W}^+$  is a concatenation of 18 different 512-dimensional  $w_i \in \mathcal{W}$  vectors, one per AdaIN layer. Clearly,  $w \in \mathcal{W}^+$  can capture richer style information than  $w' \in \mathcal{W}$ .

StyleGAN2 [22] is an improved version of StyleGAN. It makes several important changes in the generator architecture and the training strategy of StyleGAN to account for unpleasant artifacts in images generated by StyleGAN. Specifically, in StyleGAN2, each AdaIN layer is replaced with a weight demodulation, and an additional path length regularization is enforced during training. These modifications make the StyleGAN2’s generator smoother, easier to invert, and able to generate more real images than the StyleGAN’s counterpart while still retaining full controllability of style via the extended latent space  $\mathcal{W}^+$ . Therefore, unless stated otherwise, we will consider StyleGAN2 rather than StyleGAN for the rest of our paper.

### 3.2. Face Swapping with a Pretrained StyleGAN2

In the standard face swapping task, we want to transfer the identity in a source face image  $x^s$  to a target face image  $x^t$  while keeping other facial attributes (styles) in  $x^t$  unchanged. We use a well pretrained encoder  $E$  [44] to embed  $x^s$  and  $x^t$  into the latent space  $\mathcal{W}^+$  of a StyleGAN2 pretrained on face images, and derive two latent codes  $w^s$  and  $w^t \in \mathcal{W}^+$  respectively.

Motivated by the expressiveness and linear editability of  $\mathcal{W}^+$ , we argue that we can disentangle  $\mathcal{W}^+$  into two subspaces  $\mathcal{W}_{id}^+$  and  $\mathcal{W}_{sty}^+$  characterizing identity and style re-

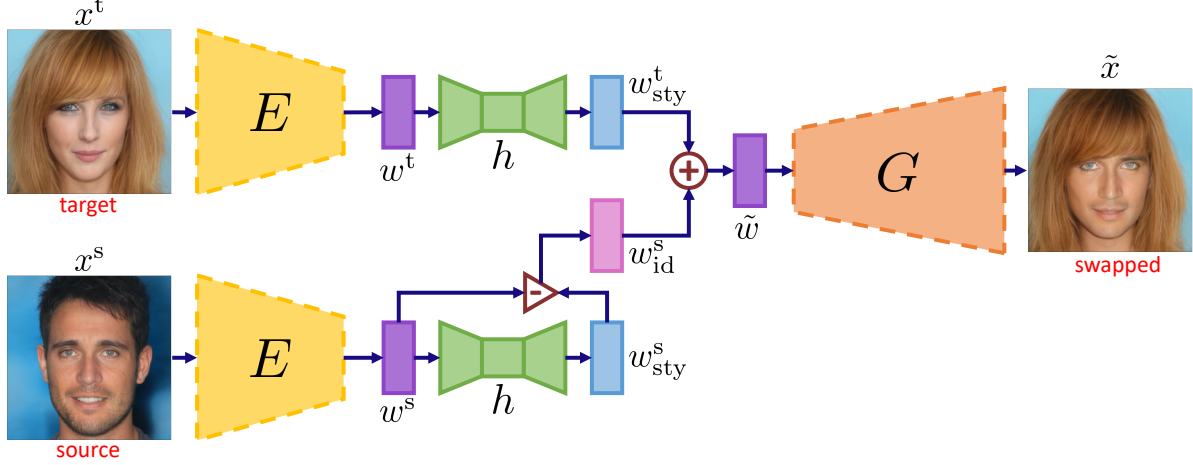


Figure 1. Overall framework of our proposed method.  $G$  is a StyleGAN2 generator,  $E$  is an encoder,  $h$  is a style extractor network. Both  $G$  and  $E$  were pretrained, thus, are marked with dashed border.

spectively, so that a latent code  $w \in \mathcal{W}^+$  can be represented as follows:

$$w = w_{\text{id}} + w_{\text{sty}} \quad (1)$$

where  $w_{\text{id}} \in \mathcal{W}_{\text{id}}^+$  and  $w_{\text{sty}} \in \mathcal{W}_{\text{sty}}^+$  denote the “identity” and “style” latent codes that capture the identity and style information in  $w$ . Similarly, we also have  $w^s = w_{\text{id}}^s + w_{\text{sty}}^s$  and  $w^t = w_{\text{id}}^t + w_{\text{sty}}^t$ .

The above arithmetic decomposition of  $w^s$  and  $w^t$  suggests an efficient and effective way to do face swapping which is adding the source identity code  $w_{\text{id}}^s$  and the target style code  $w_{\text{sty}}^t$  together:

$$\tilde{w} = w_{\text{id}}^s + w_{\text{sty}}^t \quad (2)$$

$$= w^s - w_{\text{sty}}^s + w_{\text{sty}}^t \quad (3)$$

$$= w_{\text{id}}^s + w^t - w_{\text{id}}^t \quad (4)$$

Here,  $\tilde{w}$  denotes the “swapped” latent code. We generate a swapped face image  $\tilde{x}$  from  $\tilde{w}$  by feeding  $\tilde{w}$  to the StyleGAN2 generator  $G$ , i.e.  $\tilde{x} = G(\tilde{w})$ .

Intuitively, we can generalize the face swapping in Eq. 2 to account for multiple sources and targets as follows:

$$\tilde{w} = \left( \sum_{i=1}^M \alpha_i w_{\text{id}}^{s_i} \right) + \left( \sum_{j=1}^N \beta_j w_{\text{sty}}^{t_j} \right) \quad (5)$$

$$= \sum_{i=1}^M \sum_{j=1}^N \alpha_i \beta_j \left( w_{\text{id}}^{s_i} + w_{\text{sty}}^{t_j} \right) \quad (6)$$

$$= \sum_{i=1}^M \sum_{j=1}^N \alpha_i \beta_j \tilde{w}^{s_i, t_j} \quad (7)$$

where  $M, N \geq 1$  and  $\alpha_1, \dots, \alpha_M \geq 0; \sum_{i=1}^M \alpha_i = 1$  and  $\beta_1, \dots, \beta_N \geq 0; \sum_{j=1}^N \beta_j = 1$ . The final swapped code  $\tilde{w}$  in

Eq. 7 is equivalent to the linear interpolation of individual swapped codes derived from all source-target pairs.

The remaining question is how to model  $w_{\text{id}}$  and  $w_{\text{sty}}$ . There could be various approaches to this but in our paper, we propose to learn a *style extractor network*  $h$  that maps  $w$  to  $w_{\text{sty}}$ , i.e.,  $w_{\text{sty}} = h(w)$ , and compute  $w_{\text{id}}$  as  $w_{\text{id}} = w - h(w)$ . We found this solution works well in our experiments so we leave the exploration of other approaches for future work. We can adopt  $h$  into the formula of  $\tilde{w}$  as follows:

$$\tilde{w} = w^s - h(w^s) + h(w^t) \quad (8)$$

We refer to our proposed method as “Arithmetic Face Swapping” (AFS), and provide an illustration of it in Fig. 1. Below, we provide a condition for  $h$  which ensures that  $\tilde{w}$  preserves the identity in  $w^s$ .

**Proposition 1.**  $\tilde{w}_{\text{id}} = w_{\text{id}}^s$  if and only if  $h(\tilde{w}) = h(w^t)$ .

*Proof.* Since  $\tilde{w}_{\text{id}} = \tilde{w} - h(\tilde{w}) = w_{\text{id}}^s + h(w^t) - h(\tilde{w})$ , we have  $\tilde{w}_{\text{id}} = w_{\text{id}}^s$  if and only if  $h(\tilde{w}) = h(w^t)$ .  $\square$

**Corollary 1** (Chains of face swapping operations). *If the style extractor  $h$  can preserve style for **any** face swapping operation, i.e.,  $h(\tilde{w}) = h(w^t) \forall w^s, w^t$ ; then we can perform a chain of face swapping operations without losing identity of the source image.*

*Proof.* This is just a direct extension of Prop. 1 to chains of face swapping operations and can be easily proven by induction. Below, we give an example of how it will work.

Assuming that we have performed the following chain of face swapping operations for three latent codes  $w^{(1)}, w^{(2)}, w^{(3)}$  based on the decomposition in Eq. 1:

$$\tilde{w}^{(1,2)} = w_{\text{id}}^{(1)} + w_{\text{sty}}^{(2)}$$

$$\tilde{w}^{(1,3)} = \tilde{w}_{\text{id}}^{(1,2)} + w_{\text{sty}}^{(3)}$$

Method	ID ( $\uparrow$ )	Expr. ( $\downarrow$ )	Pose ( $\downarrow$ )	FID ( $\downarrow$ )
FSGAN [30]	0.20	6.80	<b>4.31</b>	67.00
FaceShifter [27]	0.48	7.15	5.52	12.16
MegaFS [56]	0.46	8.67	6.98	11.23
AFS (Ours)	<b>0.49</b>	<b>5.01</b>	4.54	<b>4.56</b>

Table 1. Quantitative results of our face swapping method and baselines on the CelebA-HQ test set.

According to Prop. 1, if  $h(\tilde{w}^{(1,2)}) = h(w^{(2)})$ ,  $\tilde{w}_{\text{id}}^{(1,2)}$  will equal  $w_{\text{id}}^{(1)}$ ; and  $\tilde{w}^{(1,3)}$  can be written as:

$$\tilde{w}^{(1,3)} = w_{\text{id}}^{(1)} + w_{\text{sty}}^{(3)}$$

which means  $\tilde{w}^{(1,3)}$  is only composed of the identity of  $w^{(1)}$  and the style of  $w^{(3)}$  with *no* style of  $w^{(2)}$ . This allows  $h(\tilde{w}^{(1,3)})$  to be exactly similar to  $h(w^{(3)})$  and if this happens,  $\tilde{w}_{\text{id}}^{(1,3)}$  will equal  $w_{\text{id}}^{(1)}$ . The same reasoning is applied when we perform another face swapping operation between  $\tilde{w}^{(1,3)}$  and  $w^{(4)}$ .  $\square$

Given the elegance of AFS, one may wonder whether there exists a setting for  $w_{\text{id}}$ ,  $w_{\text{sty}}$ , and  $h$  so that  $\tilde{w}$  computed in Eq. 8 can faithfully preserve the source identity and the target style for any source-target pair  $(w^s, w^t)$ . In the remark below, we show that such setting exists in theory.

*Remark 1* (Possibility of AFS). If we can design  $w \in \mathbb{R}^d$  so that its first  $k$  components only capture identity and its last  $d - k$  components only capture style, and if  $h$  is a function that extracts the last  $d - k$  components of a vector, then  $\tilde{w} = w^s - h(w^s) + h(w^t)$  can faithfully preserve the source identity and the target style.

It is not hard to verify the correctness of Remark 1. Intuitively, it means we can express  $w_{\text{id}}$  as  $(w_1, \dots, w_k, 0, \dots, 0)$  and  $w_{\text{sty}}$  as  $(0, \dots, 0, w_{k+1}, \dots, w_d)$ .

Next, we will describe the objectives for training  $h$  so that  $h$  yields correct identity-style disentanglement and satisfies the style preservation condition in Prop. 1.

### 3.3. Objective Functions

**ID loss** As  $\tilde{w}$  contains the identity part of  $w^s$ , we want its generated image  $G(\tilde{w})$  will preserve the identity in the source image  $x^s$ . We define the *identity similarity score* between  $G(\tilde{w})$  and  $x^s$  as the cosine similarity between the representations computed by a pretrained ArcFace [11] model  $R$  for  $G(\tilde{w})$  and  $x^s$ , and minimize the loss below:

$$\mathcal{L}_{\text{ID}} = 1 - \cos(R(G(\tilde{w})), R(x^s)) \quad (9)$$

where  $\cos(\cdot, \cdot)$  denotes the cosine similarity.

**Feature map loss** Intermediate feature maps of a StyleGAN2 generator can be roughly divided into three groups with low ( $4 \times 4$ ,  $8 \times 8$ ), middle ( $16 \times 16$ ,  $32 \times 32$ ) and high ( $64 \times 64 \rightarrow 1024 \times 1024$ ) spatial resolutions. The first two groups have been shown to represent coarse facial attributes such as pose, face shape, and general hair style that have little effect on identity [21]. In addition, since each feature map  $i$  can be modified separately via each component  $w_i$  of a latent code  $w \in \mathcal{W}^+$ , we can force  $\tilde{w}$  to create the same style as  $w^t$  at low-resolution feature maps, leaving the identity information from  $w^s$  to be represented by high-resolution feature maps. This can be done by minimizing the loss below:

$$\mathcal{L}_{\text{feat}} = \|G_{\text{f}}(\tilde{w}) - G_{\text{f}}(w^t)\|_2 \quad (10)$$

where  $G_{\text{f}}(\cdot)$  denotes the (second)  $32 \times 32$  feature map output of the StyleGAN2 generator.

**Perceptual loss** In addition to  $\mathcal{L}_{\text{feat}}$ , we also make use of the Learned Perceptual Image Patch Similarity (LPIPS) loss [53] to enforce the perceptual similarity between  $G(\tilde{w})$  and  $x^t$ . LPIPS has been shown to account for many nuances of human perception better than other perceptual losses (e.g., SSIM [49], FSIM [52]). The formula of our LPIPS loss is given as follows:

$$\mathcal{L}_{\text{LPIPS}} = \|\text{VGG}(G(\tilde{w})) - \text{VGG}(G(w^t))\|_2 \quad (11)$$

where  $\text{VGG}(\cdot)$  denotes the feature vector extracted from a pretrained VGG [40].

**Consistency loss** To ensure  $h(\tilde{w})$  equals  $h(w^t)$  in Prop. 1, we simply minimize the L1 distance between  $h(\tilde{w})$  and  $h(w^t)$  as follows:

$$\mathcal{L}_{\text{cons}} = \|h(\tilde{w}) - h(w^t)\|_1 \quad (12)$$

**Overall loss** The overall loss function for training  $h$  is:

$$\mathcal{L} = \lambda_1 \mathcal{L}_{\text{ID}} + \lambda_2 \mathcal{L}_{\text{feat}} + \lambda_3 \mathcal{L}_{\text{LPIPS}} + \lambda_4 \mathcal{L}_{\text{cons}} \quad (13)$$

where  $\lambda_1, \lambda_2, \lambda_3, \lambda_4 \geq 0$  are coefficients. We note that we keep VGG and ArcFace intact and only train  $h$ .

### 3.4. Architecture of the Style Extractor Network

Since a latent code  $w \in \mathcal{W}^+$  has many dimensions ( $18 \times 512 = 9216$  in total), if we feed the whole latent code  $w$  to the style extractor  $h$ ,  $h$  will be very big and difficult to learn. From the observation that the components  $w_1, \dots, w_{18}$  of  $w$  can be independent of each other and usually capture different styles typical of the feature maps they control, we instead use 18 different style extractor sub-networks  $h_1, \dots, h_{18}$  for 18 different components of  $w$ . For

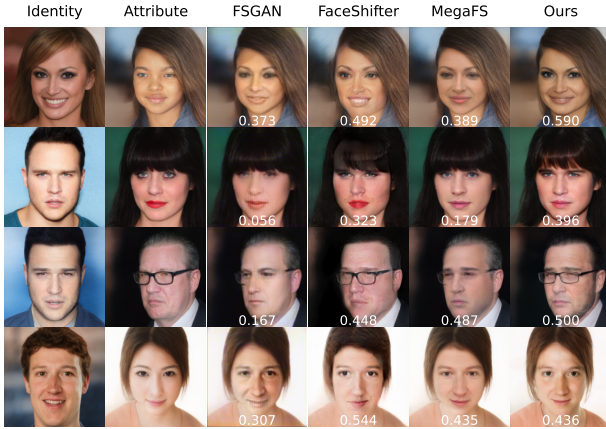


Figure 2. Visualization of swapped faces produced by our method and baselines. The first two columns contain source faces (“identity”) and target faces (“attribute”) from the CelebA-HQ test set. The identity similarity score is shown at the bottom of each swapped face image.

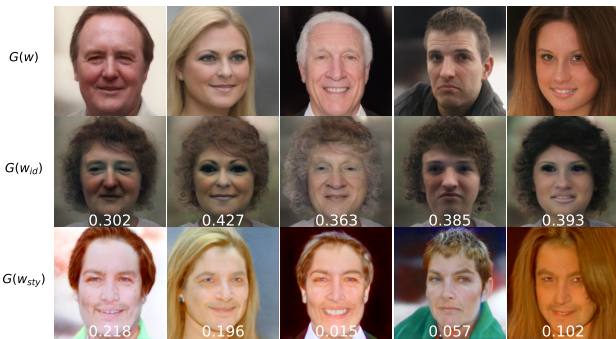


Figure 3. Visualization of the *original*, “identity”, and “style” images ( $G(w)$ ,  $G(w_{id})$ ,  $G(w_{sty})$ ) generated from the *original*, “identity” and “style” latent codes ( $w$ ,  $w_{id}$ ,  $w_{sty}$ ).

each sub-network  $h_i$ , we have the input vector of size 512 which will be transformed to a hidden vector of size 256 via a fully connected (FC) layer. Then, this hidden vector will be fed to a series of highway layers [41] before being mapped back to the size 512. By default, the number of highway layers is 2. We empirically found that this architecture facilitates the learning of  $h_i$ . We tried to replace the highway layers with standard FC layers but achieved worse results. We hypothesize that maybe the gating mechanism in highway layers facilitate selecting which elements of  $w_i$  should be discarded and retained to get the correct style code component.

## 4. Experiments

### 4.1. Experimental Setup

#### 4.1.1 Datasets and training settings

We used the CelebA-HQ dataset [20] for our experiments. This dataset contains 30k celebrities’ faces at megapixel resolutions ( $1024 \times 1024$ ) and is challenging for face swapping. We used a pretrained e4e encoder [44] to invert 27176 images in the training and validation sets of CelebA-HQ to latent codes, and trained our style extractor  $h$  on these latent codes. We trained  $h$  for 10 epochs with a batch size of 4. We used an Adam optimizer with an initial learning rate of  $1e-4$ , decayed to  $1e-6$  following a cosine schedule over all steps. We set the loss coefficients (Eq. 13) as follows:  $\lambda_1=1$ ,  $\lambda_2=3.5$ ,  $\lambda_3=1$ , and  $\lambda_4=0.1$ .

#### 4.1.2 Metrics

For identity preservation evaluation, we use the *identity similarity score* which is the cosine similarity produced by a pretrained ArcFace [11] for  $\tilde{x}$  and  $x^s$ . We follow previous works [27, 56] and consider *pose* and *expression* for attribute preservation evaluation. The *expression error* is the L2 distance between 2D landmarks of  $\tilde{x}$  and  $x^t$  which are extracted by the Face Alignment library<sup>1</sup>. The *pose error* is the L2 distance between the outputs of Hopenet [37] w.r.t.  $\tilde{x}$  and  $x^t$ . We computed the identity similarity score, expression error, pose error on 5000 source-target pairs sampled randomly from the test set of CelebA-HQ. To measure the visual quality of swapped faces, we use the Fréchet Inception Distance (FID) [18]. We formed 15k source-target pairs from 30k images of CelebA-HQ and generated 15k swapped faces from these pairs. We computed the FID between the swapped faces images and the original images of CelebA-HQ.

### 4.2. Main Results

#### 4.2.1 Quantitative comparison

As shown in Table 1, AFS outperforms all face swapping baselines in all metrics except for the case in which ours achieves a higher pose error than FSGAN. This means the swapped faces generated by our method not only have better visual quality but also preserve the source identity and target attributes better than those generated by the baselines, which justifies the effectiveness of our arithmetic identity-style disentanglement of the latent space  $\mathcal{W}^+$  for face swapping. For the case that AFS has higher pose error than FSGAN, we think the possible reason is that FSGAN explicitly models the target pose (via its 3DMM) and uses this information for face swapping while our method does not. However, since FSGAN does not use GAN to generate swapped

<sup>1</sup><https://github.com/ladrianb/face-alignment>

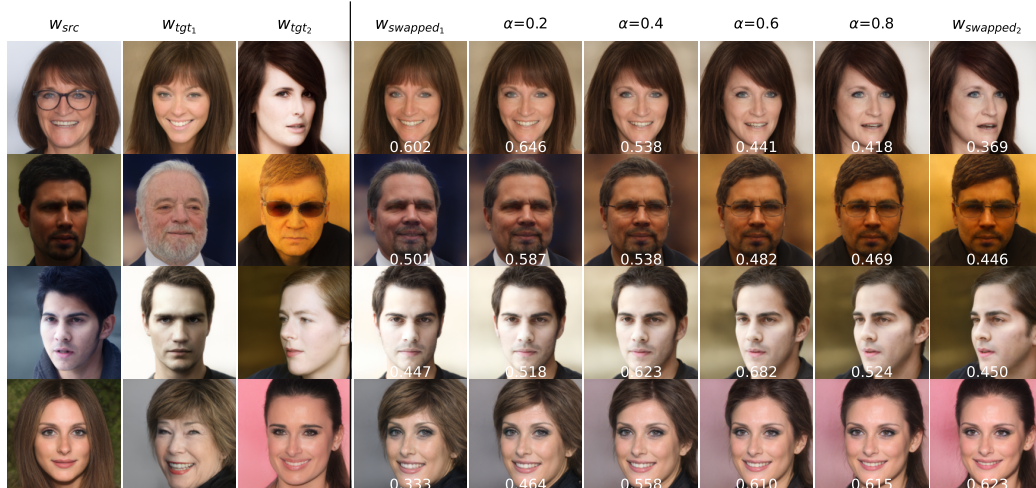


Figure 4. Results of combining an identity from one source ( $w^s$ ) with styles from two targets ( $w^1, w^2$ ). The formula of the final swapped latent code  $\tilde{w}$  is  $\tilde{w} = w_{id}^s + (\alpha w_{sty}^1 + (1 - \alpha)w_{sty}^2)$  with  $0 \leq \alpha \leq 1$ .

faces, it achieves a very poor FID score compared to ours and other GAN-based baselines.

#### 4.2.2 Visualization of swapped faces

As shown in Fig. 2, the swapped faces generated by AFS look more natural and detailed than those generated by the baselines, which reflects the low FID score of our method in Table 1. Since FSGAN and MegaFS apply the target face mask to the swapped result to keep the hair and background of the target face image intact, it is not surprising that their swapped faces look exactly similar to the target face in all details except for the face region specified by the face mask. However, simply using face masks as a postprocessing step can lead to some unwanted artifacts, e.g., when the target subject wears eyeglasses (row 3). Our method, despite not using face masks, still preserves the target attributes very well. FaceShifter also does this well since it only adjusts certain areas in the target feature maps specified by the source identity embedding vector in a selective manner. However, FaceShifter often produces artifacts when the source and target faces have largely different shapes (row 1 and row 4) while our method does not have such problem.

#### 4.2.3 Visualization of identity and style latent codes

One interesting capability of AFS that may not be found in other face swapping methods is the visualization of identity and style codes. Fig. 3 shows some examples of “identity” and “style” images ( $G(w_{id}), G(w_{sty})$ ) generated from the corresponding identity and style codes ( $w_{id}, w_{sty}$ ), respectively. All these images are interpretable faces, which empirically verifies that  $w_{id}$  and  $w_{sty}$  are in the subspaces of  $\mathcal{W}^+$  rather than some arbitrary spaces. The “identity”

images have almost the same general styles (e.g., straight-looking, brown curly hair, pale skin) and only differ in some identity-specific facial attributes (e.g., eye shape, nose shape, cheek type) which, we think, are considered useful by the face recognition model  $R$ . By contrast, the “style” images seem to have similar identities, and are mainly different in identity-unrelated facial attributes (e.g., hair style and color, skin color, shirt color). These results indicate that our method properly disentangles a latent code into identity and style parts, and is, to some extent, more interpretable than existing methods.

#### 4.2.4 Face swapping with one identity and two styles

In Fig. 4, we show face swapping results with an identity from one source and styles from two targets. The contribution of each target to the final result is controlled via a hyperparameter  $\alpha$  ( $0 \leq \alpha \leq 1$ ). Clearly, the style of the final swapped face is a linear interpolation of the styles of two individual swapped faces, which empirically justifies our formula in Eq. 7. We also note that there is a slight difference in the identity similarity scores of the two individual swapped faces. It implies that the target style has some effect on the output of the face recognition model  $R$ .

#### 4.2.5 Chains of face swapping operations

In the Method section, we theoretically showed that our method is able to perform chains of face swapping operations if  $h$  satisfies the condition in Cor. 1 which is characterized by the loss  $\mathcal{L}_{cons}$  (Eq. 12). In this experiment, we empirically verify this capability. From Fig. 5, it is clear that adding  $\mathcal{L}_{cons}$  to the final loss greatly improves the performance of our method, allowing our method to

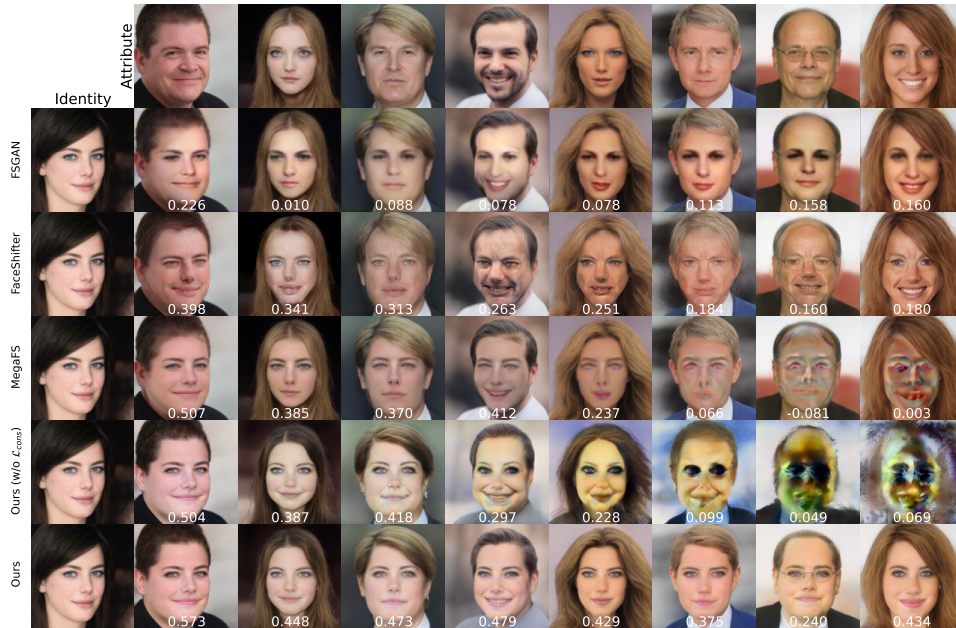


Figure 5. Results of running a chain of face swapping operations. The leftmost column shows a single source face, and the topmost row shows multiple target faces that will be used sequentially for face swapping. Each of the following rows shows a sequence of swapped faces generated by each method. Each swapped face in the sequence is derived from the face *immediately to the left* as source and the face *at the topmost row* as target. The identity similarity score between a swapped face and the original source face (leftmost) is shown at the bottom of the swapped face image.

generate high-fidelity swapped faces that well preserve the source identity and target attributes even after many successive steps of face swapping. Meanwhile, FaceShifter and MegaFS start producing unnatural swapped faces after just two and four steps, respectively.

#### 4.2.6 Other results

Due to space limit, we refer readers to the Appendix for results on “face swapping with two identities and one style”, and on “semantically meaningful linear transformations in the identity and style spaces”.

### 5. Conclusion

We have proposed a novel high-fidelity face swapping method called “Arithmetic Face Swapping” (AFS) that disentangles the intermediate latent space  $\mathcal{W}^+$  of a pretrained StyleGAN2 into two subspaces w.r.t. the identity and style, and treats face swapping as an arithmetic operation in this space, i.e., the summation of a source identity code and a target style code. Our method can easily generalize over the standard face swapping to support multiple source identities and target styles. Extensive experiments have demonstrated the advantages of our method in generating high-quality swapped faces over several SOTAs. In the future, we would like to examine different architectures of  $h$  and

different training objectives that lead to better preservation of the source identity and target attributes.

## 6. Ethical Considerations

### 6.1. General Ethical Conduct

The CelebA-HQ dataset [20] is available for non-commercial research purposes. When using this dataset, we adhere to the agreements specified by the dataset owners<sup>2</sup>. Since the data we used are only human face images with no identity or facial attribute annotations, and since the face images are publicly available on the Internet, it is unlikely that these data reveal any personally identifiable information such as name, age, sex, etc., or contain private, sensitive information that could be degrading or embarrassing for some people.

### 6.2. Potential Negative Societal Impacts

Our proposed method is aimed to be a simple yet effective method for face swapping that could be widely applied to the entertainment industry and identity-concealing tasks. Despite these good purposes, our method may be misused to cause societal harms. Some potential scenarios are:

1. Counterfeiting a picture of a person  $A$  doing bad things

<sup>2</sup><https://mmlab.ie.cuhk.edu.hk/projects/CelebA.html>



by swapping the identity of the true person in the picture with that of  $A$  to damage the reputation of  $A$ .

2. Creating a face with a non-existing identity (e.g., face swapping with multiple identities) and use this identity to do frauds without being tracked by the authorities.

The first scenario raises a harassment concern while the second one raises a security concern. Both scenarios are difficult to mitigate and tend to be more serious when our proposed method becomes better. For the first scenario, a possible solution is building a framework that allows face swapping only if the target image contains no actions that break the social and moral norms. For the second scenario, one solution is maintaining a database of all known faces for verifying whether a given face exists in the database or not.

## References

- [1] Rameen Abdal, Yipeng Qin, and Peter Wonka. Image2stylegan: How to embed images into the stylegan latent space? In *Proceedings of the IEEE/CVF International Conference on Computer Vision*, pages 4432–4441, 2019. 1, 2, 3
- [2] Rameen Abdal, Yipeng Qin, and Peter Wonka. Image2stylegan++: How to edit the embedded images? In *Proceedings of the IEEE/CVF Conference on Computer Vision and Pattern Recognition*, pages 8296–8305, 2020. 1, 3
- [3] Alexander A Alemi, Ian Fischer, Joshua V Dillon, and Kevin Murphy. Deep variational information bottleneck. *arXiv preprint arXiv:1612.00410*, 2016. 2
- [4] Jianmin Bao, Dong Chen, Fang Wen, Houqiang Li, and Gang Hua. Towards open-set identity preserving face synthesis. In *Proceedings of the IEEE conference on computer vision and pattern recognition*, pages 6713–6722, 2018. 1, 2
- [5] David Bau, Jun-Yan Zhu, Jonas Wulff, William Peebles, Hendrik Strobelt, Bolei Zhou, and Antonio Torralba. Seeing what a gan cannot generate. In *Proceedings of the IEEE/CVF International Conference on Computer Vision*, pages 4502–4511, 2019. 3
- [6] Dmitri Bitouk, Neeraj Kumar, Samreen Dhillon, Peter Belhumeur, and Shree K Nayar. Face swapping: automatically replacing faces in photographs. In *ACM SIGGRAPH 2008 papers*, pages 1–8. 2008. 1, 2
- [7] Volker Blanz, Kristina Scherbaum, Thomas Vetter, and Hans-Peter Seidel. Exchanging faces in images. In *Computer Graphics Forum*, volume 23, pages 669–676. Wiley Online Library, 2004. 2
- [8] Andrew Brock, Jeff Donahue, and Karen Simonyan. Large scale gan training for high fidelity natural image synthesis. *arXiv preprint arXiv:1809.11096*, 2018. 1
- [9] Renwang Chen, Xuanhong Chen, Bingbing Ni, and Yanhao Ge. Simswap: An efficient framework for high fidelity face swapping. In *Proceedings of the 28th ACM International Conference on Multimedia*, pages 2003–2011, 2020. 1, 2
- [10] Antonia Creswell and Anil Anthony Bharath. Inverting the generator of a generative adversarial network. *IEEE transactions on neural networks and learning systems*, 30(7):1967–1974, 2018. 3
- [11] Jiankang Deng, Jia Guo, Niannan Xue, and Stefanos Zafeiriou. Arcface: Additive angular margin loss for deep face recognition. In *Proceedings of the IEEE/CVF conference on computer vision and pattern recognition*, pages 4690–4699, 2019. 5, 6
- [12] Yu Deng, Jiaolong Yang, Sicheng Xu, Dong Chen, Yunde Jia, and Xin Tong. Accurate 3d face reconstruction with weakly-supervised learning: From single image to image set. In *Proceedings of the IEEE/CVF Conference on Computer Vision and Pattern Recognition Workshops*, pages 0–0, 2019. 2
- [13] Vincent Dumoulin, Jonathon Shlens, and Manjunath Kudlur. A learned representation for artistic style. *arXiv preprint arXiv:1610.07629*, 2016. 3
- [14] Gege Gao, Huaibo Huang, Chaoyou Fu, Zhaoyang Li, and Ran He. Information bottleneck disentanglement for identity swapping. In *Proceedings of the IEEE/CVF conference on computer vision and pattern recognition*, pages 3404–3413, 2021. 2
- [15] Golnaz Ghiasi, Honglak Lee, Manjunath Kudlur, Vincent Dumoulin, and Jonathon Shlens. Exploring the structure of a real-time, arbitrary neural artistic stylization network. *arXiv preprint arXiv:1705.06830*, 2017. 3
- [16] Ian Goodfellow, Jean Pouget-Abadie, Mehdi Mirza, Bing Xu, David Warde-Farley, Sherjil Ozair, Aaron Courville, and Yoshua Bengio. Generative adversarial nets. *Advances in neural information processing systems*, 27, 2014. 1, 2, 3
- [17] Erik Härkönen, Aaron Hertzmann, Jaakko Lehtinen, and Sylvain Paris. Ganspace: Discovering interpretable gan controls. *Advances in Neural Information Processing Systems*, 33:9841–9850, 2020. 3, 12
- [18] Martin Heusel, Hubert Ramsauer, Thomas Unterthiner, Bernhard Nessler, and Sepp Hochreiter. Gans trained by a two time-scale update rule converge to a local nash equilibrium. *Advances in neural information processing systems*, 30, 2017. 6
- [19] Xun Huang and Serge Belongie. Arbitrary style transfer in real-time with adaptive instance normalization. In *Proceedings of the IEEE international conference on computer vision*, pages 1501–1510, 2017. 2, 3

- [20] Tero Karras, Timo Aila, Samuli Laine, and Jaakko Lehtinen. Progressive growing of gans for improved quality, stability, and variation. *arXiv preprint arXiv:1710.10196*, 2017. [1](#), [6](#), [8](#)
- [21] Tero Karras, Samuli Laine, and Timo Aila. A style-based generator architecture for generative adversarial networks. In *Proceedings of the IEEE/CVF conference on computer vision and pattern recognition*, pages 4401–4410, 2019. [1](#), [3](#), [5](#)
- [22] Tero Karras, Samuli Laine, Miika Aittala, Janne Hellsten, Jaakko Lehtinen, and Timo Aila. Analyzing and improving the image quality of stylegan. In *Proceedings of the IEEE/CVF conference on computer vision and pattern recognition*, pages 8110–8119, 2020. [1](#), [3](#)
- [23] Ira Kemelmacher-Shlizerman. Transfiguring portraits. *ACM Transactions on Graphics (TOG)*, 35(4):1–8, 2016. [1](#)
- [24] Diederik P Kingma and Max Welling. Auto-encoding variational bayes. *arXiv preprint arXiv:1312.6114*, 2013. [2](#)
- [25] Iryna Korshunova, Wenzhe Shi, Joni Dambre, and Lucas Theis. Fast face-swap using convolutional neural networks. In *Proceedings of the IEEE international conference on computer vision*, pages 3677–3685, 2017. [1](#), [2](#)
- [26] Jia Li, Zhaoyang Li, Jie Cao, Xingguang Song, and Ran He. Facepainter: High fidelity face adaptation to heterogeneous domains. In *Proceedings of the IEEE/CVF conference on computer vision and pattern recognition*, pages 5089–5098, 2021. [2](#)
- [27] Lingzhi Li, Jianmin Bao, Hao Yang, Dong Chen, and Fang Wen. Faceshifter: Towards high fidelity and occlusion aware face swapping. *arXiv preprint arXiv:1912.13457*, 2019. [1](#), [2](#), [5](#), [6](#)
- [28] Zachary C Lipton and Subarna Tripathi. Precise recovery of latent vectors from generative adversarial networks. *arXiv preprint arXiv:1702.04782*, 2017. [3](#)
- [29] Ryota Natsume, Tatsuya Yatagawa, and Shigeo Morishima. Fsnnet: An identity-aware generative model for image-based face swapping. In *Asian Conference on Computer Vision*, pages 117–132. Springer, 2018. [2](#)
- [30] Yuval Nirkin, Yosi Keller, and Tal Hassner. Fsgan: Subject agnostic face swapping and reenactment. In *Proceedings of the IEEE/CVF international conference on computer vision*, pages 7184–7193, 2019. [1](#), [2](#), [5](#)
- [31] Yuval Nirkin, Iacopo Masi, Anh Tran Tuan, Tal Hassner, and Gerard Medioni. On face segmentation, face swapping, and face perception. In *2018 13th IEEE International Conference on Automatic Face & Gesture Recognition (FG 2018)*, pages 98–105. IEEE, 2018. [1](#), [2](#)
- [32] Pascal Paysan, Reinhard Knothe, Brian Amberg, Sami Romdhani, and Thomas Vetter. A 3d face model for pose and illumination invariant face recognition. In *2009 sixth IEEE international conference on advanced video and signal based surveillance*, pages 296–301. Ieee, 2009. [2](#)
- [33] Guim Perarnau, Joost Van De Weijer, Bogdan Raducanu, and Jose M Álvarez. Invertible conditional gans for image editing. *arXiv preprint arXiv:1611.06355*, 2016. [3](#)
- [34] Patrick Pérez, Michel Gangnet, and Andrew Blake. Poisson image editing. In *ACM SIGGRAPH 2003 Papers*, pages 313–318. 2003. [2](#)
- [35] Elad Richardson, Yuval Alaluf, Or Patashnik, Yotam Nitzan, Yaniv Azar, Stav Shapiro, and Daniel Cohen-Or. Encoding in style: a stylegan encoder for image-to-image translation. In *Proceedings of the IEEE/CVF conference on computer vision and pattern recognition*, pages 2287–2296, 2021. [3](#)
- [36] Andreas Rossler, Davide Cozzolino, Luisa Verdoliva, Christian Riess, Justus Thies, and Matthias Nießner. Faceforensics++: Learning to detect manipulated facial images. In *Proceedings of the IEEE/CVF international conference on computer vision*, pages 1–11, 2019. [1](#), [2](#)
- [37] Nataniel Ruiz, Eunji Chong, and James M Rehg. Fine-grained head pose estimation without keypoints. In *Proceedings of the IEEE conference on computer vision and pattern recognition workshops*, pages 2074–2083, 2018. [6](#)
- [38] Yujun Shen, Ceyuan Yang, Xiaoou Tang, and Bolei Zhou. Interfacegan: Interpreting the disentangled face representation learned by gans. *IEEE transactions on pattern analysis and machine intelligence*, 2020. [3](#)
- [39] Yujun Shen and Bolei Zhou. Closed-form factorization of latent semantics in gans. In *Proceedings of the IEEE/CVF Conference on Computer Vision and Pattern Recognition*, pages 1532–1540, 2021. [3](#)
- [40] Karen Simonyan and Andrew Zisserman. Very deep convolutional networks for large-scale image recognition. *arXiv preprint arXiv:1409.1556*, 2014. [5](#)
- [41] Rupesh K Srivastava, Klaus Greff, and Jürgen Schmidhuber. Training very deep networks. *Advances in neural information processing systems*, 28, 2015. [6](#)
- [42] Ayush Tewari, Mohamed Elgharib, Florian Bernard, Hans-Peter Seidel, Patrick Pérez, Michael Zollhöfer, and Christian Theobalt. Pie: Portrait image embedding for semantic control. *ACM Transactions on Graphics (TOG)*, 39(6):1–14, 2020. [3](#)

- [43] Ayush Tewari, Mohamed Elgharib, Gaurav Bharaj, Florian Bernard, Hans-Peter Seidel, Patrick Pérez, Michael Zollhofer, and Christian Theobalt. Stylerig: Rigging stylegan for 3d control over portrait images. In *Proceedings of the IEEE/CVF Conference on Computer Vision and Pattern Recognition*, pages 6142–6151, 2020. 3
- [44] Omer Tov, Yuval Alaluf, Yotam Nitzan, Or Patashnik, and Daniel Cohen-Or. Designing an encoder for stylegan image manipulation. *ACM Transactions on Graphics (TOG)*, 40(4):1–14, 2021. 2, 3, 6
- [45] Dmitry Ulyanov, Vadim Lebedev, Andrea Vedaldi, and Victor Lempitsky. Texture networks: Feed-forward synthesis of textures and stylized images. *arXiv preprint arXiv:1603.03417*, 2016. 2
- [46] Andrey Voynov and Artem Babenko. Unsupervised discovery of interpretable directions in the gan latent space. In *International conference on machine learning*, pages 9786–9796. PMLR, 2020. 3
- [47] Hong-Xia Wang, Chunhong Pan, Haifeng Gong, and Huai-Yu Wu. Facial image composition based on active appearance model. In *2008 IEEE International Conference on Acoustics, Speech and Signal Processing*, pages 893–896. IEEE, 2008. 2
- [48] Yuhan Wang, Xu Chen, Junwei Zhu, Wenqing Chu, Ying Tai, Chengjie Wang, Jilin Li, Yongjian Wu, Feiyue Huang, and Rongrong Ji. Hiface: 3d shape and semantic prior guided high fidelity face swapping. *arXiv preprint arXiv:2106.09965*, 2021. 2
- [49] Zhou Wang, Alan C Bovik, Hamid R Sheikh, and Eero P Simoncelli. Image quality assessment: from error visibility to structural similarity. *IEEE transactions on image processing*, 13(4):600–612, 2004. 5
- [50] Yangyang Xu, Bailin Deng, Junle Wang, Yanqing Jing, Jia Pan, and Shengfeng He. High-resolution face swapping via latent semantics disentanglement. In *Proceedings of the IEEE/CVF Conference on Computer Vision and Pattern Recognition*, pages 7642–7651, 2022. 1, 3
- [51] Guoxing Yang, Nanyi Fei, Mingyu Ding, Guangzhen Liu, Zhiwu Lu, and Tao Xiang. L2m-gan: Learning to manipulate latent space semantics for facial attribute editing. In *Proceedings of the IEEE/CVF Conference on Computer Vision and Pattern Recognition*, pages 2951–2960, 2021. 3
- [52] Lin Zhang, Lei Zhang, Xuanqin Mou, and David Zhang. Fsim: A feature similarity index for image quality assessment. *IEEE transactions on Image Processing*, 20(8):2378–2386, 2011. 5
- [53] Richard Zhang, Phillip Isola, Alexei A Efros, Eli Shechtman, and Oliver Wang. The unreasonable effectiveness of deep features as a perceptual metric. In *CVPR*, 2018. 5
- [54] Jiapeng Zhu, Yujun Shen, Deli Zhao, and Bolei Zhou. In-domain gan inversion for real image editing. In *European conference on computer vision*, pages 592–608. Springer, 2020. 3
- [55] Xiangyu Zhu, Zhen Lei, Xiaoming Liu, Hailin Shi, and Stan Z Li. Face alignment across large poses: A 3d solution. In *Proceedings of the IEEE conference on computer vision and pattern recognition*, pages 146–155, 2016. 2
- [56] Yuhao Zhu, Qi Li, Jian Wang, Cheng-Zhong Xu, and Zhenan Sun. One shot face swapping on megapixels. In *Proceedings of the IEEE/CVF Conference on Computer Vision and Pattern Recognition*, pages 4834–4844, 2021. 1, 3, 5, 6

Feat. layer	ID ( $\uparrow$ )	Expr. ( $\downarrow$ )	Pose ( $\downarrow$ )	FID ( $\downarrow$ )
convs.3	0.56	7.75	8.29	5.10
<i>convs.5</i>	<i>0.49</i>	<i>5.01</i>	<i>4.54</i>	<i>4.56</i>
convs.7	0.46	4.00	3.43	4.32

Table 2. Quantitative results with different feature layers for computing  $\mathcal{L}_{\text{feat}}$  (Eq. 10). convs.3, convs.5, convs.7 have feature maps of size  $16 \times 16$ ,  $32 \times 32$ ,  $64 \times 64$ , respectively. The default feature layer is convs.5 highlighted in *italic*.

## A. Appendix

### A.1. Ablation Studies

#### A.1.1 Using different feature layers of the StyleGAN2 generator

Table 2 shows the quantitative results when different feature layers are used for computing  $\mathcal{L}_{\text{feat}}$ . We keep all the loss coefficients as default. We observe that there is a clear trade-off between style and identity preservation. As we use a deeper layer for our loss (convs.7), the identity similarity decreases while the preservation of expression and pose is better. This is expected as using deeper layer will force the  $\tilde{w}$  close to  $w^t$ . By contrast, using lower layer (convs.3) will cause style to be not well preserved. The best feature layer, in our opinion, is convs.5.

#### A.1.2 Contributions of the loss components

In Fig. 6, we show the qualitative results of our method without  $\mathcal{L}_{\text{feat}}$  or  $\mathcal{L}_{\text{LPIPS}}$  to examine the contribution of each loss term. Apparently, without  $\mathcal{L}_{\text{feat}}$ , our method fails to preserve the general shape of the target face. Meanwhile, without  $\mathcal{L}_{\text{LPIPS}}$ , our method fails to maintain the skin color and illumination of the target face. Therefore, we need both  $\mathcal{L}_{\text{feat}}$  and  $\mathcal{L}_{\text{LPIPS}}$  to achieve good results.

### A.2. Other Results

#### A.2.1 More qualitative face swapping results

We provide more qualitative results of our method in Fig. 7. Overall, our method preserves the source identity and the target styles quite well, and can handle occlusions such as wearing glasses. However, there are cases in which AFS produces undesirable results. For example, our method is unable to preserve the skin texture of the target face if it is very different from the counterpart of the source face.

#### A.2.2 Face swapping with two identities and one style

In Fig. 8, we show some results of combining the identities of two sources with the style of one target. The hyperparameter  $\alpha$  ( $0 \leq \alpha \leq 1$ ) controls how much the two sources affect the final results. When  $\alpha$  varies in  $[0, 1]$ , we can

clearly see the identity of the final swapped face interpolates between the identities of two individual swapped faces while the style of the final swapped face remains almost unchanged. These results, again, empirically validate our formula in Eq. 7. They also indicate that our method truly separates the identity from styles.

#### A.2.3 Scaling identity and style latent codes

In Figs. 9 and 10, we visualize swapped faces with the style code and the identity code being scaled, respectively. It is clear that the swapped faces do not look real when the style code or the identity code are scaled with negative or very large  $\alpha$ . This means the swapped latent code  $\tilde{w}$  in these cases no longer resides in the latent space  $\mathcal{W}^+$ . Negative  $\alpha$  causes  $\tilde{w}$  to be much more off-the-space- $\mathcal{W}^+$  than very large  $\alpha$ . Scaling style codes leads to the decrease in identity similarity scores since the swapped code  $\tilde{w}$  is now dominated by the scaled style code  $\alpha w_{\text{sty}}$ . By contrast, scaling identity codes cause the identity similarity to change slightly, sometimes even increase compared to not scaling. This means i) the swapped code  $\tilde{w}$  is now dominated by the scaled identity code  $\alpha w_{\text{id}}$ , and ii) the identity code computed by our method truly reflects the identity specified by the face recognition model  $R$ .

#### A.2.4 Semantically meaningful linear transformations in the identity and style spaces

In this subsection, we empirically examine that with our arithmetic decomposition of  $\mathcal{W}^+$  into the identity and style subspaces, whether we can perform linear transformation in one subspace without affecting the other or not. Mathematically, it means whether  $(w_{\text{id}} + \alpha \Delta_{\text{id}}) + w_{\text{sty}}$  still has the same styles as  $w_{\text{id}} + w_{\text{sty}}$  or not ( $\alpha \in \mathbb{R}$ ,  $\Delta_{\text{id}}$  is a semantically meaningful editing direction in  $\mathcal{W}_{\text{id}}^+$ ). Note that this only holds true if  $\mathcal{W}_{\text{id}}^+$  and  $\mathcal{W}_{\text{sty}}^+$  are fully disentangled as specified in Remark 1. Otherwise, we can write  $(w_{\text{id}} + \alpha \Delta_{\text{id}}) + w_{\text{sty}}$  as  $w_{\text{id}} + (\alpha \Delta_{\text{id}} + w_{\text{sty}})$ , and thus,  $w_{\text{sty}}$  will be affected by  $\alpha \Delta_{\text{id}}$ .

We follow the strategy in GANSpace [17] to find a set of editing directions  $\{\Delta_{\text{id}}\}$  ( $\{\Delta_{\text{sty}}\}$ ) in  $\mathcal{W}_{\text{id}}^+$  ( $\mathcal{W}_{\text{sty}}^+$ ). Specifically, we compute the principal components from the identity (style) latent codes of the training face images via PCA, and regard these principal components as editing directions. In Fig. 11 (Fig. 12), we show the top three principal components in  $\mathcal{W}_{\text{id}}^+$  ( $\mathcal{W}_{\text{sty}}^+$ ). We observe that gender, age, skin color are factors that cause large changes of identity while hair styles, viewpoints, wearing glasses are those that cause large changes of style. We also see that changing style does not affect identity much in terms of visual perception (Fig. 12), which suggests that our method can effectively separate identity from style.



Figure 6. Qualitative results of our method without  $\mathcal{L}_{feat}$  or  $\mathcal{L}_{LPIPS}$ .



Figure 7. More face swapping results of our method with applied masks.

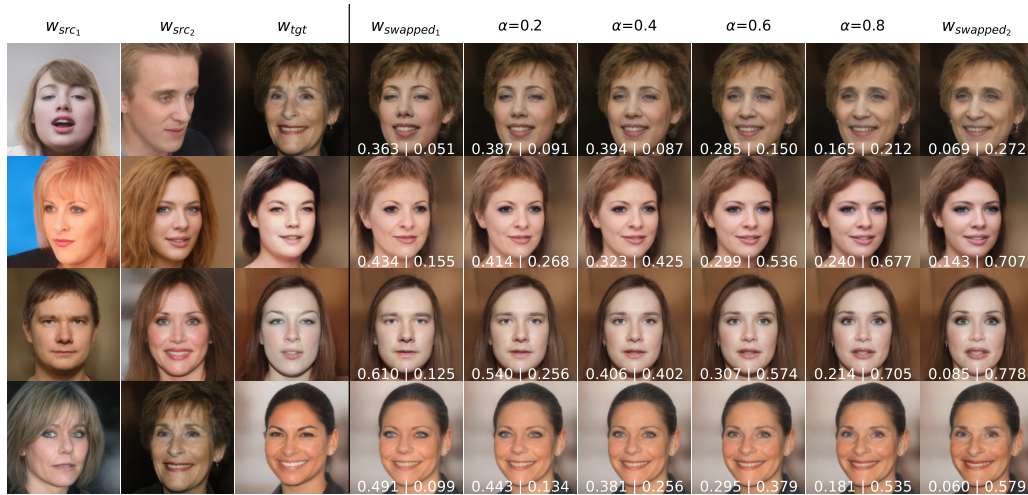


Figure 8. Results of combining the identities of two sources ( $w^{s_1}$ ,  $w^{s_2}$ ) with the style of one target ( $w^t$ ). The formula of the final swapped latent code  $\tilde{w}$  is  $\tilde{w} = (\alpha w_{id}^{s_1} + (1 - \alpha)w_{id}^{s_2}) + w_{sty}^t$  with  $0 \leq \alpha \leq 1$ . Under each swapped image, we show two identity similarity scores. The left one corresponds to the first source, and the right one corresponds to the second source.

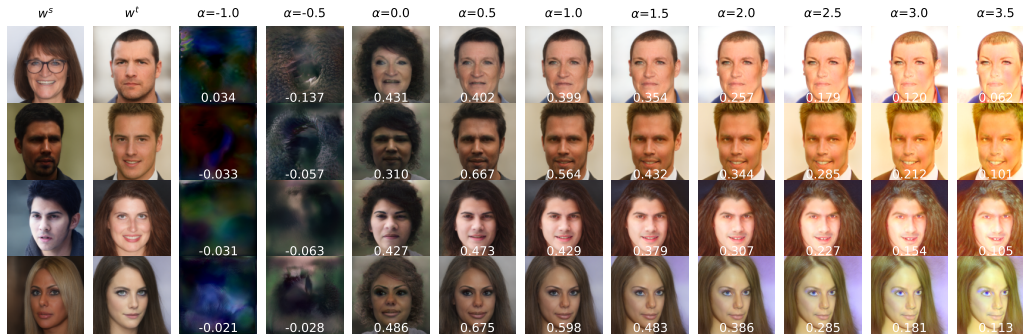


Figure 9. Generated swapped faces when the style code is scaled by  $\alpha$ . The formula of the swapped latent code is  $\tilde{w} = w_{id} + \alpha w_{sty}$ . The identity similarity score is shown under each swapped image.

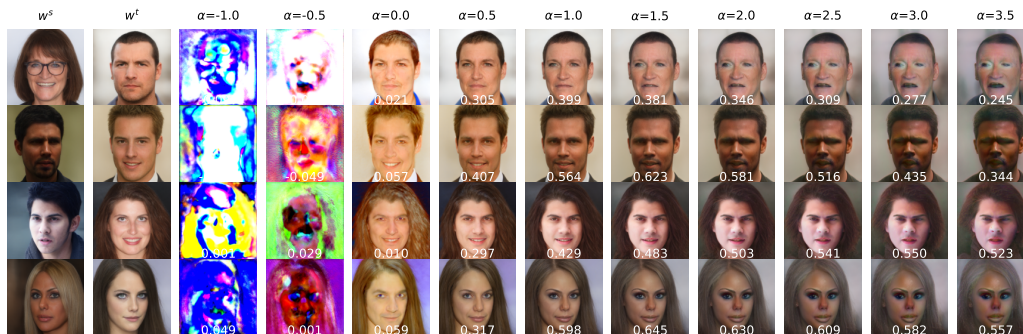


Figure 10. Generated swapped faces when the identity code is scaled by  $\alpha$ . The formula of the swapped latent code is  $\tilde{w} = \alpha w_{id} + w_{sty}$ . The identity similarity score is shown under each swapped image.

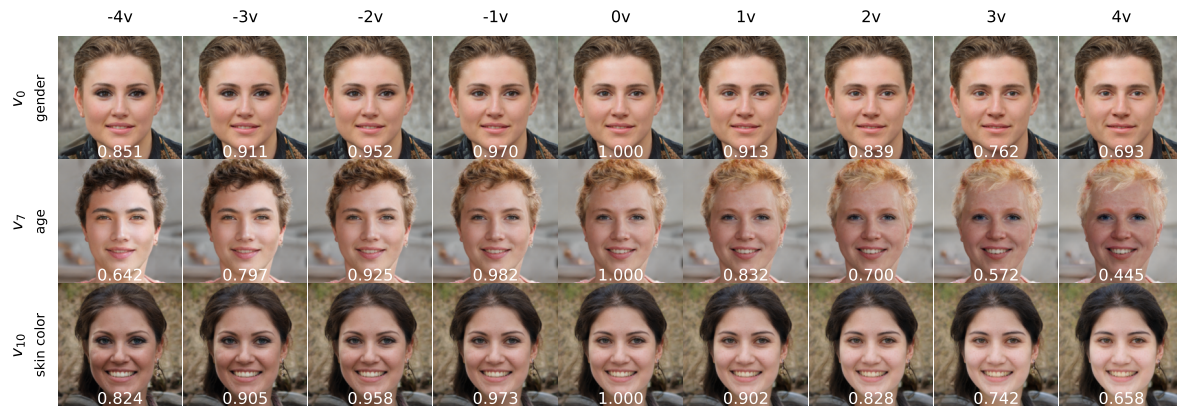


Figure 11. The top three principal components in the identity space  $\mathcal{W}_{id}^+$ .

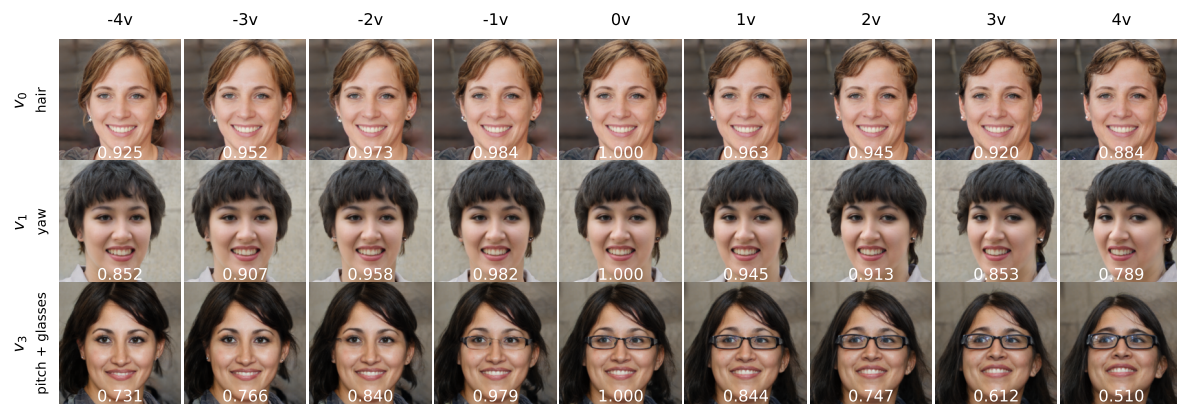


Figure 12. The top three principal components in the style space  $\mathcal{W}_{sty}^+$ .